

ASYMMETRIC DRIFT AND THE STELLAR VELOCITY ELLIPSOID

Kyle B. Westfall¹, Matthew A. Bershad¹, Marc A. W. Verheijen²,
David R. Andersen³, & Rob A. Swaters⁴

¹*University of Wisconsin – Madison,* ²*Kapteyn Institute,*

³*NRC Herzberg Institute of Astrophysics,* ⁴*University of Maryland*

Abstract

We present the decomposition of the stellar velocity ellipsoid using stellar velocity dispersions within a 40° wedge about the major-axis (σ_{maj}), the epicycle approximation, and the asymmetric drift equation. Thus, we employ no fitted forms for σ_{maj} and escape interpolation errors resulting from comparisons of the major and minor axes. We apply the theoretical construction of the method to integral field data taken for NGC 3949 and NGC 3982. We derive the vertical-to-radial velocity dispersion ratio (σ_z/σ_R) and find (1) our decomposition method is accurate and reasonable, (2) NGC 3982 appears to be rather typical of an Sb type galaxy with $\sigma_z/\sigma_R = 0.73^{+0.13}_{-0.11}$ despite its high surface brightness and small size, and (3) NGC 3949 has a hot disk with $\sigma_z/\sigma_R = 1.18^{+0.36}_{-0.28}$.

1. Motivation and Methodology

The shape of the stellar velocity ellipsoid, defined by σ_R , σ_ϕ , and σ_z , provides key insights into the dynamical state of a galactic disk: $\sigma_z:\sigma_R$ provides a measure of disk heating and $\sigma_\phi:\sigma_R$ yields a check on the validity of the epicycle approximation (EA). Additionally, σ_R is a key component in measuring the stability criterion and in correcting rotation curves for asymmetric drift (AD), while σ_z is required for measuring the disk mass-to-light ratio. The latter is where the DiskMass survey focuses (Verheijen et al. 2004, 2005); however, in anything but face-on systems, σ_z must be extracted via decomposition of the line-of-sight (LOS) velocity dispersion. Below, we present such a decomposition for two galaxies in the DiskMass sample: NGC 3949 and NGC 3982.

Previous long-slit studies (e.g., Shapiro et al. 2003 and references therein) acquired observations along the major and minor axes and performed the decomposition via the EA and AD equations; using both dynamical equations overspecifies the problem such that AD is often used as a consistency check. Here, use of the SparsePak (Bershad et al. 2004, 2005) integral field unit (IFU) automatically provides multiple position angles, thereby increasing ob-

serving efficiency and ensuring signal extraction along the desired kinematic axes. Long-slit studies have also used functional forms to reduce the sensitivity of the above decomposition method to noise. Here, only measures of the LOS velocity dispersions within a 40° wedge about the major axis are used to perform the decomposition by incorporating both the EA and AD equations under some simplifying assumptions. Velocities and radii within the wedge are projected onto the major axis according to derived disk inclinations, i , and assuming near circular motion. In the end, our method requires neither fitted forms nor error-prone interpolation between the major and minor axes. Future work will compare this decomposition method with the multi-axis long-slit method and investigate effects due to use of points off the kinematic axes.

Following derivations in Binney & Tremaine (1987) and assuming (1) EA holds, (2) the velocity ellipsoid shape and orientation is independent of z ($\partial(\overline{v_R v_z})/\partial z = 0$), (3) both the space density, ν , and σ_R have an exponential fall off radially with scale lengths of h_R and $2h_R$, respectively, and (4) the circular velocity is well-represented by the gaseous velocity, v_g , the equation for the AD of the stars becomes $v_g^2 - \overline{v_*^2} = \frac{1}{2}\sigma_R^2 \left(\frac{\partial \ln \overline{v_*}}{\partial \ln R} + 4\frac{R}{h_R} - 1 \right)$, where $\overline{v_*}$ is the mean stellar rotation velocity; hence, σ_R is the only unknown. The third assumption requires mass to follow light, $\Sigma \propto \sigma_z^2$, and constant velocity ellipsoid axis ratios with radius; Σ is the surface density. The major-axis dispersion is geometrically given by $\sigma_{maj}^2 = \sigma_\phi^2 \sin^2 i + (\eta \sigma_R)^2 \cos^2 i$, where $\eta = \sigma_z / \sigma_R$ is constant with radius. Finally, EA, $\sigma_\phi^2 / \sigma_R^2 = \frac{1}{2} \left(\frac{\partial \ln \overline{v_*}}{\partial \ln R} + 1 \right)$, completes a full set of equations for decomposition of the velocity ellipsoid.

2. Analysis

Data for testing of the above formalism was obtained during SparsePak commissioning (Bershady et al. 2005, see Table 1). Both NGC 3949 and NGC 3982 were observed for 3×2700 s at one IFU position with $\lambda_c = 513.1$ nm and $\lambda/\Delta\lambda = 11700$ or 26 km s^{-1} . The velocity distribution function (VDF) of both gas and stars is parameterized by a Gaussian function. In each fiber with sufficient signal-to-noise, the gaseous VDF is extracted using fits to the [OIII] emission line; the stellar VDF is extracted using a modified cross-correlation method (Tonry & Davis 1979; Statler 1995) with HR 7615 (K0III) as the template (Westfall et al. 2005). The pointing of the IFU on the galaxy is determined *post factum* to better than $1''$ by minimizing the χ^2 difference between the fiber continuum flux and the surface brightness profile. Subsequent galactic coordinates have been deprojected according to the kinematic i and position angle.

Figure 1 shows LOS dispersions for both the gas, $\sigma_{g,LOS}$, and stars, $\sigma_{*,LOS}$; data points are given across the full field of the IFU with points along the major and minor axes and in between having different symbols (see caption). From

this Figure note (1) there is no significant difference in σ_{LOS} along the major and minor axes for NGC 3949 and (2) the large gas dispersion within $R \leq 10''$ for NGC 3982 is a result of poor single Gaussian fits to the multiple dynamical components of its LINER nucleus.

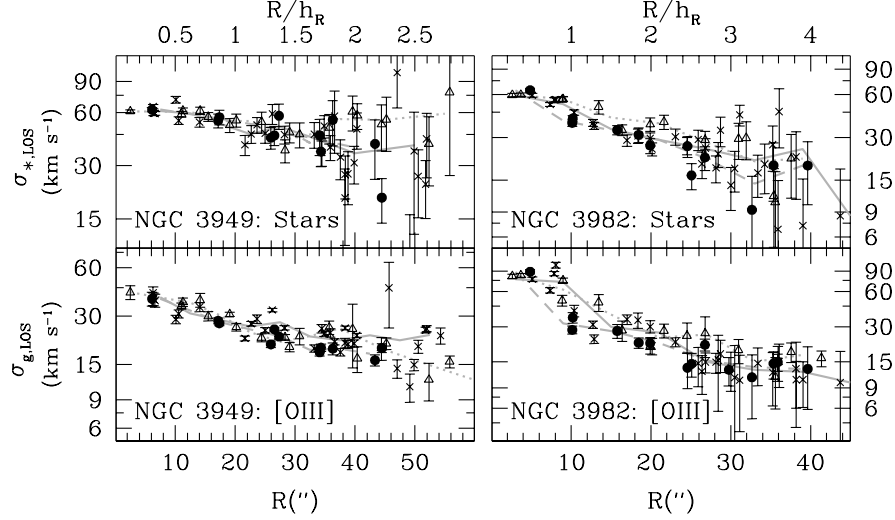


Figure 1. Measurements of the LOS dispersions in NGC 3949 (left) and NGC 3982 (right) for stars (top) and gas (bottom) as a function of galactic radius; the top axis is in units of scale length (h_R is 20 and 10 arcsec in NGC 3949 and NGC 3982, respectively). Major axis, minor axis, and in between fibers are shown as points, triangles, and crosses, respectively; “axis fibers” lie in a 40° wedge around the axis. The binned mean values are shown for the major axis, minor axis, and otherwise as dashed, dotted, and solid lines, respectively.

Figure 2 gives the folded gaseous and stellar rotation curves and compares the measured σ_{maj} from Figure 1 with that calculated using the formalism from §1. The value of η used in Figure 2 provides the minimum difference between the two sets of data (as measured by χ^2_ν ; see Figure 3a). We find $\eta = 1.18^{+0.36}_{-0.28}$ and $\eta = 0.73^{+0.13}_{-0.11}$ for NGC 3949 and NGC 3982, respectively; errors are given by 68% confidence limits. A comparison of these values to the summary in Shapiro et al. (2003) is shown in Figure 3b. The disk of NGC 3982 is similar to other Sb types studied; however, NGC 3949 seems to have an inordinately hot disk. The latter, while peculiar, is also supported by the indifference between its major and minor axis σ_{LOS} from Figure 1 and the same indifference seen in the CaII data presented by Bershadsky et al. (2002). Our streamlined velocity-ellipsoid decomposition method appears accurate, as seen by comparison with (1) galaxies of a similar type for NGC 3982, and (2) data in a different spectral region for NGC 3949.

This work was generously supported by an AAS International Travel Grant, the Wisconsin Space Grant Consortium, and the NSF Grant AST-0307417.

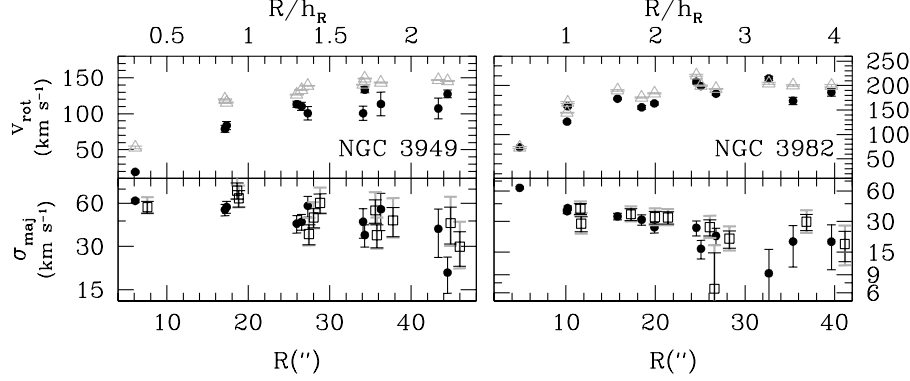


Figure 2. Comparison of measured and calculated σ_{maj} in NGC 3949 (left) and NGC 3982 (right). Top panels show the deprojected rotational velocity for both the gas (grey triangles) and stars (black points) along the major axis. Bottom panels compare the measured σ_{maj} (points) to those from our formalism using η as derived from Figure 3a (squares; offset in R for comparison). Errors on σ_{maj} are also calculated when using the 68% confidence limits for η (grey).

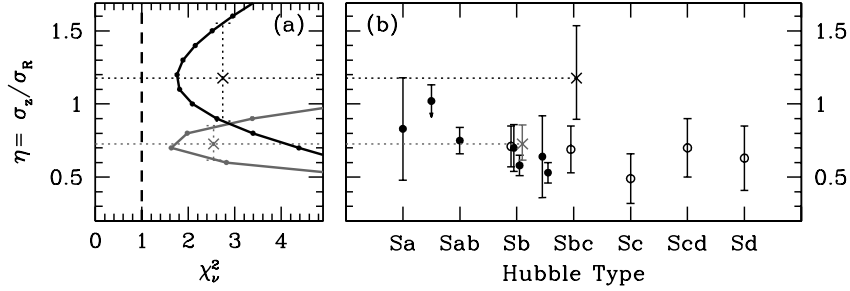


Figure 3. Derivation of the ratio $\eta = \sigma_z/\sigma_R$. In (a), the χ^2_ν statistic is used to find the best correspondence between the model and measured data sets for NGC 3949 (black line) and NGC 3982 (grey line). The 68% (1 σ) confidence limits on η are determined by an increase of χ^2_ν by 1 (dotted lines). The disk heating of NGC 3949 (black cross) and NGC 3982 (grey cross) are placed on Figure 5 from Shapiro et al. (2003) in (b).

References

- Bershady, M., Verheijen, M., Andersen, D. 2002, in *Disks of Galaxies: Kinematics, Dynamics and Perturbations*, eds. E. Athanassoula & A. Bosma, ASP Conference Series, 275, 43
- Bershady, M. A. et al. 2004, *PASP*, 116, 565
- Bershady, M. A. et al. 2005, *ApJS*, 156, 311
- Binney, J. & Tremaine, S. 1987, *Galactic Dynamics* (Princeton University Press: Princeton, NJ)
- Shapiro, K. L., Gerssen, J., & van der Marel, R. P. 2003, *AJ*, 126, 2707
- Staler, T. 1995, *AJ*, 109, 1371
- Tonry, J. & Davis, M. 1979, *AJ*, 84, 1511
- Verheijen, M. A. W. et al. 2004, *AN*, 325, 151
- Verheijen, M. et al. 2005, these proceedings
- Westfall, K. B. et al. 2005, in prep.